# Three-dimensional self-assembly using dipolar interaction

Leon Abelmann[1,2*], Tijmen A.G. Hageman[1,2], Per A. Löthman[1,2],
Massimo Mastrangeli[3], Miko C. Elwenspoek[2]

[1] KIST Europe, Saarland University, Saarbrücken, Germany

[2] University of Twente, The Netherlands

[3] Electronic Components, Technology and Materials, Department of Microelectronics, Delft University of Technology, The Netherlands

*l.abelmann@utwente.nl

**Abstract:**

Interaction between dipolar forces, such as permanent magnets, generally leads to the formation of one-dimensional chains and rings. We investigated whether it was possible to let dipoles self-assemble into three-dimensional structures by encapsulating them in a shell with a specific shape. We discovered that the condition for self-assembly of a three-dimensional crystal is satisfied when the energies of dipoles in the parallel and anti-parallel states are equal. Our experiments show that the most regular structures are formed by using cylinders and cuboids, and not by spheroids. This simple design rule will help the self-assembly community to realise three-dimensional crystals from objects in the micrometre range, which opens up the way towards novel meta-materials.

**One Sentence Summary:**

Magnets with the correct shape spontaneously grow into three-dimensional crystals.

## Introduction

Crystal growth is a form of self-assembly (*1–3*), where the individual objects (atoms, molecules) arrange into regular arrays. The process of crystal formation has been studied in great detail (*4*) on a vast range of materials, and has a widespread technological impact ranging from silicon single crystals (*5*) for the semiconductor industry to diffraction studies on proteins (*6*). Crystal growth takes place by a nucleation and growth mechanism. Nucleation starts on well-defined templates (epitaxy) (*7*), random imperfections (formation of snowflakes), or occurs spontaneously in space (*8*). The latter is the subject of this study.

Crystal formation of objects larger than atoms and molecules is receiving increasing attention (*9*, *10*), driven by the promise of meta-materials with novel functionality (*11*, *12*). There are beautiful examples of crystal growth from silica or polymer spheres, such as for 3D photonic crystals (*13–15*). In these examples, the self-assembly process relies on the evaporation of a solvent to bring the components in each other's vicinity, possibly assisted by solvent flow (*16*). In simulations, the increase in particle concentration is often modelled by slowly contracting the simulation space (*17*). Alternatively, self-assembly can be driven by sedimentation (*18*). These approaches generally lead to close-packed structures (*10*). After solvent evaporation, the assembly is held together by Van der Waals forces between particles or by residues from the solvent (cementing) (*19*). Van der Waals forces act over a short range and become less effective

for larger objects. Therefore, long-range static forces are being investigated, such as in a binary mixture of oppositely charged spheres (*20*).

When growing crystals of identical objects, the objects themselves obviously cannot have a net charge. On the microscale, one can use induced or permanent dipoles, which could either be of electrostatic or magnetic origin (*21*). The dipole moments can be either induced by an externally applied field (*22*, *23*) or they can be permanent. In this study, we investigate the possibility of self-assembling crystals using permanent magnetic dipolar forces. Permanent magnetic dipoles are especially useful for objects of large size, since magnetic poles are not easily screened. What we learn in this way from magnetic dipoles can be applied to electric dipoles, since long range forces between both types of dipoles are identical.

Magnetic dipoles allow us to increase the object size to the millimetre range (*24*). At this scale, it is easy to study the process of three-dimensional self-assembly in real time. By doing so, we not only obtain information on the final product of self-assembly, but also on the processes that lead to the formation of the assembly. Real time observation of the self-assembly process provides clues on the origin of defects.

We performed experiments with millimetre sized permanent magnets, embedded in a polymer shell of varying shape. The objects were submerged in water, in a transparent conical cylinder with an inner diameter ranging from 9 to 19 cm (Fig. 1A). Gravitational forces were counterbalanced by an upward water flow that decreased in speed due to the conical shape of the boundary, so that the objects remain in the field of view of the camera. The adjustable turbulence in the flow created disturbing forces to enable the system to reach the global energy minimum. These disturbing forces provide stochastic kinetic energy to the objects, leading to a motion analogous to Brownian motion (*25*).

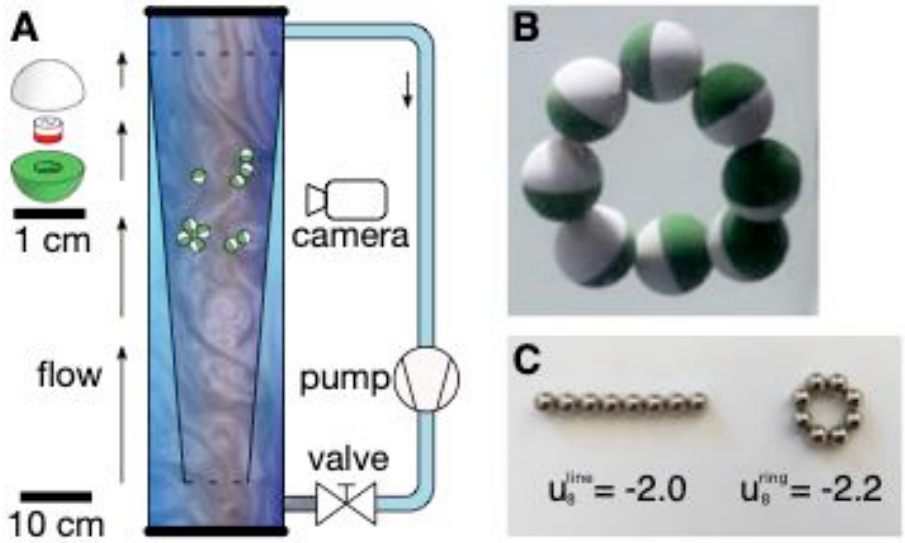


**Fig. 1.** The self-assembly experiment. **(A)** 3D printed polymer objects with embedded permanent magnets were inserted in a transparent cylinder with an upward flow. The flow counteracts the drop velocity of the objects, and the flow's turbulence provides a disturbing force. A tapered transparent insert was used to provide a gradient in the flow velocity, which ensured that the objects levitate in front of the video cameras. **(B)** Spherical objects form linear

chains. When eight spheres are inserted in the flow, the most stable configuration is a circle, which has 10% lower energy than a linear chain **(C).**

The interaction between permanent spherical dipoles results in the formation of chains (*26*). Fig. 1B shows an example with eight dipoles that line up in a ring. The formation of these rings is well understood (*27–29*). The dipolar forces first organise the spheres into a line. The energy of this configuration, relative to the energy of a dipole pair ($N = 2$), is:

$$u_N^{\text{line}} = \frac{-2}{N}\sum_{i=1}^{N-1}\frac{N-i}{i^3}$$

For more than three spheres, a lower energy state can be reached by closing the line into a ring:

$$u_N^{\text{ring}} = \frac{-1}{4}\sin^3\left(\frac{\pi}{N}\right)\sum_{k=1}^{N-1}\frac{3+\cos(2\pi k/N)}{\sin^3(\pi k/N)}$$

In case of eight spheres the energy gain is substantial (Fig. 1C), so the ring forms easily and remains intact.

These one-dimensional chains form because the anti-parallel dipole configuration has twice the energy of the parallel configuration at identical dipole centre-to-centre distance (Fig. 2A, left). To achieve assemblies with higher dimensionality, we can use the shape of the polymer shell to change the distance between the dipoles for different orientations. By elongating the shell, we can increase the distance between the dipole centres in the parallel configuration to the point that the energy of the anti-parallel configuration is lower than the parallel configuration. In this case the anti-parallel configuration is preferred and we obtain two-dimensional plate-like structures (Fig. 2A, centre). If the energies of the parallel and anti-parallel states are equal, newly arriving dipoles align both in a parallel and an anti-parallel fashion and one would expect three-dimensional structures (Fig. 2A, right).

## Results

We demonstrated this strategy for eight spheroids, cylinders, and cuboids. The energy difference between the anti-parallel and parallel states was chosen to be 40 μJ for all shapes (Fig. 2B, first column). As predicted, we observe the formation of line structures. Only a spherical shell allows the formation of a ring. Cylinders and cubes form rigid lines. For the cubes, this is in agreement with molecular dynamics studies and experiments on iron nanocubes prepared in a gas phase cluster gun (*30*) By reversing the energy difference between the parallel and anti-parallel states, so that the anti-parallel state has the lowest energy (Fig. 2B, centre column), we observed clear plate structures for the cylinders, less perfect plates for the cuboids, and irregular structures for the spheroids. When both energies were equal (Fig. 2B, third column), the cylinders started to form perfect three-dimensional 2x2x2 clusters (red circle in Fig. 2B) The cuboids' assemblies suffered from relatively stable attachments of cuboids at a 90₀ orientation, which led to magnetic flux closure and prohibited further growth. The spheroids formed a complex double ring structure, which resembled the prediction made by Messina for larger numbers of objects (*29*).

In our experiment, the structures of spheroids stay together for several minutes. This is much longer than is the case for the structures of cylinders and cubes, which often break up into parts after a few seconds. The ring structure of spheres breaks up rather easily into a chain, but then

reconnects again into a ring in less than a minute. We believe the higher stability of the spheroid structures is caused by their ability to misalign without immediately increasing their distance, which decreases the force between the magnets. In general, the chain structures break up more easily (within a few seconds) than the plates or crystals. This is expected since breaking a chain only requires to break a single bond between two objects, whereas for plates and crystals multiple bonds need to be broken simultaneously. Additionally, the cylinders and cubes form rigid chains that are very long, resulting in frequent contact with the reactor walls and breaking of the chain.

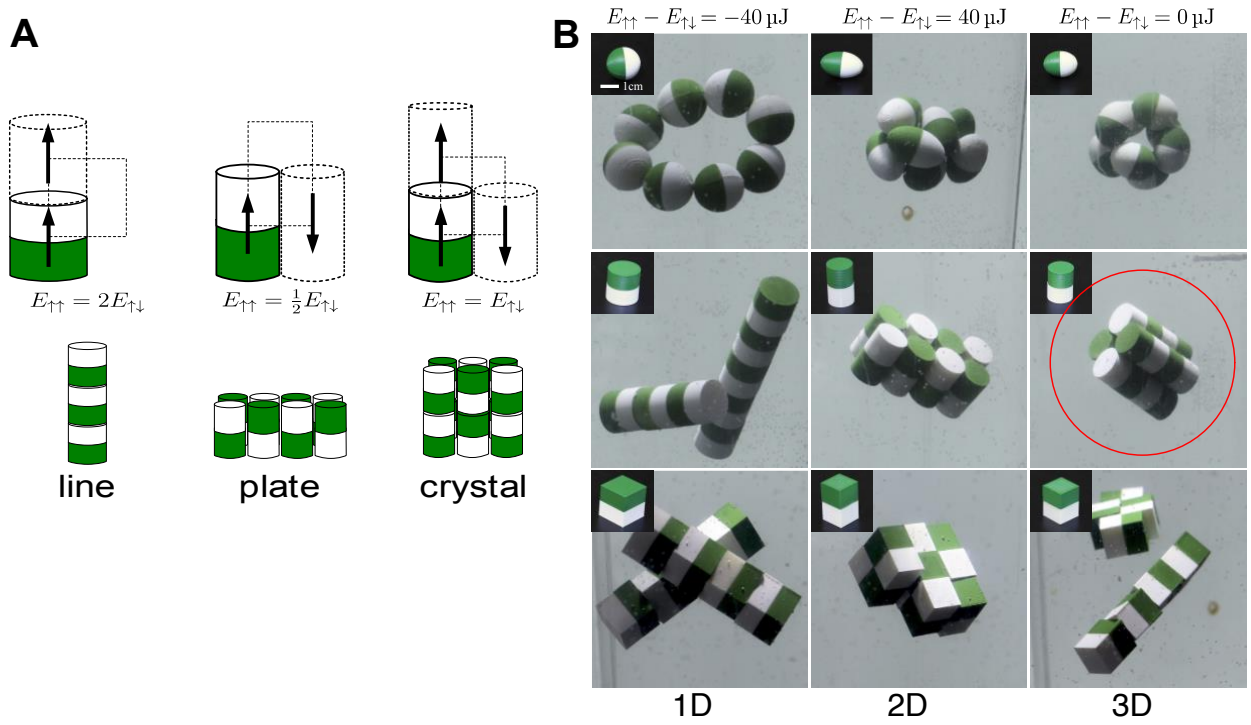


**Fig. 2.** Three-dimensional self-assembly of dipoles. **(A)** Equally spaced dipoles prefer parallel alignment (black arrows). By elongating the shape of the shell around the dipoles, we can favour the anti-parallel configuration, so that plates of objects assemble. When the energy of the parallel and anti-parallel configuration is exactly equal, we expect three-dimensional crystals. **(B)** This strategy works best with cylindrical objects. From left to right we varied the shape so that the energy of the parallel configuration is twice (left), half (centre), and exactly equal (right) to that of the anti-parallel configuration. The red encircled assembly of cylinders (middle row) is a regular three-dimensional 2x2x2 cluster. The cylindrical objects in the second row reproduced the plate prediction of figure **(A)**. The spheroids (top row) and the cubes (bottom row) exhibited line structures in the first column, but more complex behaviour when their shape was adjusted.

Out of the shapes we investigated, cylinders appear to be most suited for self-assembly into well-defined three-dimensional structures. Experiments with an increasing number of objects (Fig. S1), confirmed that spheroids do not form regular crystals, in contrast to cylinders and cuboids. Insights as to why this happens can be obtained by studying the process of self-assembly itself (videos S1 and S2 in supplementary material). The spheroids tend to stay together longer as a cluster than the cylinders and cuboids. Clusters of cylinders and cuboids often break up into two smaller clusters, which then realign to form a more regular crystal.

The break-up of assemblies happens more often for larger assemblies, probably because shear forces tend to increase with assembly size. This effect might be amplified by our former observation that the energy in the turbulent flow increases with increasing length scale (*25*). We are not sure whether this is a general aspect of turbulent driven self-assembly, or a particular aspect of our experimental configuration. This question needs further investigation, for instance by changing the absolute size of the objects.

Especially single cylinders attached to the cluster can wander rather easily over the surface, which is not the case for cuboids. The cuboids take a longer time to attach to each other. We suspect that to fully adhere, the water between the cuboids needs to be pushed out over a few millimetres. In the case of spheroids and cylinders, the amount of water to be displaced is far less.

## Discussion

These experiments demonstrate that three-dimensional structures can self-assemble from dipolar forces, provided that there is no preference for parallel or anti-parallel alignment. This can be achieved by balancing dipolar forces with steric interactions induced by the specific shape of the object. It is interesting that the shape of the object plays such a major role. The spheroids have many orientations under which they can attach to a forming cluster, the cuboids on the other hand only have a few. The cylindrical shape appears to be a good compromise. Also, in 2D self-assembly it was shown that a rounded shape helps to achieve regular crystals (*31*).

As well as the energy difference between the final states, the paths towards those energy minima are also of major importance. This observation is in agreement with molecular dynamic simulations, which show that spheres are more likely to form larger clusters than cubes (*32*) and that dipolar interaction disturbs the formation of crystal formation of cubes (*33*).

These results encourage experiments on self-assembly of crystals at the microscale using permanent magnetic dipoles. The millimetre sized cylindrical objects could be miniaturised by lithographic techniques and anisotropic etching on magnetic thin films with a perpendicular easy axis sandwiched between two non-magnetic films, such as is currently used in magnetic random access memories(*34*). From there, one can envision interesting meta-materials, such as artificial anti-ferromagnets, piezo-magnetic materials with a negative Poisson ratio (*11*), or three-dimensional magnetic ring-core memories (*35*).

The forces between dipoles do not change when we reduce the size of the dipoles, apart from a scaling factor. Neither does it matter whether the dipoles are of magnetic or electrical origin. This implies that we can generalise the outcome of these experiments to the design of electrostatically interacting objects of micrometre size for three-dimensional self-assembly, aimed at applications such as photonic crystals(*14*), supermaterials(*11*), three-dimensional electronics (*36*), or memories (*35*).

## Materials and Methods

The experimental setup was introduced and characterised in (*24*, *25*). New to this setup was a cone-shaped inset, which created a flow gradient meant to centre particles in the middle and prevent interaction with the top and bottom. The 3D printed shells are either spheroids, cylinders, or cuboid, ordered in increasing extent to which the particle poses geometrical restrictions on how they can connect. All objects have an identical cylindrical, 4x4 mm axially-magnetized

NdFeB core, and are colour-coded based on polarisation. They are designed such that $E_{ax}-E_{diam} \in \{-40,0,40\}$ μJ, in order of increasing aspect ratio, while ensuring that their minimum connection energy stays at −80 μJ. The 3D design files (STL format) for the shells are available as supplementary material. The dimensions of the objects, measured with a calliper, are listed in table S1. Objects in various amounts (8, 12, 16) were inserted into the reactor with appropriate flow speed (approximately 9 cm/s) settings to create neutral buoyancy.

**References and Notes:**

1. G. M. Whitesides, B. Grzybowski, Self-assembly at all scales. *Science (80-. ).* **295**, 2418–2421 (2002).
2. G. Singh, H. Chan, A. Baskin, E. Gelman, N. Repnin, P. Kràl, R. Klajn, Self-assembly of magnetite nanocubes into helical superstructures. *Science (80-. ).* **345**, 1149 (2014).
3. N. Bowden, A. Terfort, J. Carbeck, G. M. Whitesides, Assembly of mesoscale objects into ordered two-dimensional arrays. *Science (80-. ).* **276**, 233–235 (1997).
4. J. S. Langer, Instabilities and pattern formation in crystal growth. *Rev. Mod. Phys.* **52**, 1–28 (1980).
5. K. M. Beatty, K. A. Jackson, Monte Carlo modeling of silicon crystal growth. *J. Cryst. Growth*. **211**, 13–17 (2000).
6. D. S. Goodsell, A. J. Olson, Structural Symmetry and Protein Function. *Annu. Rev. Biophys. Biomol. Struct.* **29**, 105–153 (2000).
7. I. Bita, J. K. W. Yang, Y. S. Jung, C. A. Ross, E. L. Thomas, K. K. Berggren, Graphoepitaxy of Self-Assembled Block Copolymers on Two-Dimensional Periodic Patterned Templates. *Science (80-. ).* **321**, 939–943 (2008).
8. J. L. Katz, H. Wiedersich, Nucleation theory without Maxwell Demons. *J. Colloid Interface Sci.* **61**, 351–355 (1977).
9. V. Liljeström, C. Chen, P. Dommersnes, J. O. Fossum, A. H. Gröschel, Active structuring of colloids through field-driven self-assembly. *Curr. Opin. Colloid Interface Sci.* **40**, 25–41 (2019).
10. X. Bouju, É. Duguet, F. Gauffre, C. R. Henry, M. L. Kahn, P. Mélinon, S. Ravaine, Nonisotropic Self-Assembly of Nanoparticles: From Compact Packing to Functional Aggregates. *Adv. Mater.* **30**, 1706558 (2018).
11. M. Elwenspoek, L. Abelmann, E. Berenschot, J. van Honschoten, H. Jansen, N. Tas, Self-assembly of (sub-)micron particles into supermaterials. *J. Micromech. Microeng.* **20**, 64001 (2010).
12. J. D. Joannopoulos, Self-assembly lights up. *Nature*. **414**, 257–258 (2001).
13. A. van Blaaderen, R. R., P. Wiltzius, Template-directed colloidal crystallization. *Nature*. **385**, 321–323 (1997).
14. Y. A. Vlasov, X.-Z. Bo, J. C. Sturm, D. J. Norris, On-chip natural assembly of silicon photonic bandgap crystals. *Nature*. **414**, 289–293 (2001).
15. N. V Dziomkina, M. A. Hempenius, G. J. Vancso, Towards true 3-dimensional BCC

colloidal crystals with controlled lattice orientation. *Polymer (Guildf).* **50**, 5713–5719 (2009).

16. D. J. Norris, E. G. Arlinghaus, L. Meng, R. Heiny, L. E. Scriven, Opaline photonic crystals: How does self-assembly work? *Adv. Mater.* **16**, 1393-1399+1385 (2004).
17. P. F. Damasceno, M. Engel, S. C. Glotzer, Predictive Self-Assembly of Polyhedra into Complex Structures. *Science (80-. ).* **337**, 453–457 (2012).
18. J. Henzie, M. Grünwald, A. Widmer-Cooper, P. L. Geissler, P. Yang, Self-assembly of uniform polyhedral silver nanocrystals into densest packings and exotic~superlattices. *Nat. Mater.* **11**, 131–137 (2011).
19. R. van Dommelen, P. Fanzio, L. Sasso, Surface self-assembly of colloidal crystals for micro- and nano-patterning. *Adv. Colloid Interface Sci.* **251**, 97–114 (2018).
20. M. E. Leunissen, C. G. Christova, A.-P. Hynninen, C. P. Royall, A. I. Campbell, A. Imhof, M. Dijkstra, R. Van Roij, A. Van Blaaderen, Ionic colloidal crystals of oppositely charged particles. *Nature*. **437**, 235–240 (2005).
21. K. J. M. Bishop, C. E. Wilmer, S. Soh, B. A. Grzybowski, Nanoscale Forces and Their Uses in Self-Assembly. *Small*. **5**, 1600–1630 (2009).
22. F. Ilievski, K. A. Mirica, A. K. Ellerbee, G. M. Whitesides, Templated self-assembly in three dimensions using magnetic levitation. *Soft Matter*. **7**, 9113–9118 (2011).
23. L. A. Woldering, A. J. Been, L. Alink, L. Abelmann, Using magnetic levitation for {2D} and {3D} self-assembly of cubic silicon macroparticles. *Phys. status solidi RRL*. **10**, 176–184 (2016).
24. T. A. G. Hageman, P. A. Löthman, M. Dirnberger, M. Elwenspoek, A. Manz, L. Abelmann, Macroscopic equivalence for microscopic motion in a turbulence driven three-dimensional self-assembly reactor. *J. Appl. Phys.* **123**, 24901 (2018).
25. P. A. Löthman, T. A. G. Hageman, M. C. Elwenspoek, G. J. M. Krijnen, M. Mastrangeli, A. Manz, L. Abelmann, A Thermodynamic Description of Turbulence as a Source of Stochastic Kinetic Energy for 3D Self-Assembly. *Adv. Mater. Interfaces*. **1900963**, 1–11 (2019).
26. B. Bian, G. Chen, Q. Zheng, J. Du, H. Lu, J. P. Liu, Y. Hu, Z. Zhang, Self-Assembly of {CoPt} Magnetic Nanoparticle Arrays and its Underlying Forces. *Small*. **14**, 1801184 (2018).
27. R. Messina, I. Stankovic, Self-assembly of magnetic spheres in two dimensions: The relevance of onion-like structures. *EPL (Europhysics Lett.* **110** (2015).
28. G. I. Vega-Bellido, R. A. DeLaCruz-Araujo, I. Kretzschmar, U. M. Córdova-Figueroa, Self-assembly of magnetic colloids with shifted dipoles. *Soft Matter*. **15**, 4078–4086 (2019).
29. R. Messina, L. A. Khalil, I. Stankovic, Self-assembly of magnetic balls: From chains to tubes. *Phys. Rev. E - Stat. Nonlinear, Soft Matter Phys.* **89** (2014).
30. L. Balcells, I. Stanković, Z. Konstantinović, A. Alagh, V. Fuentes, L. López-Mir, J. Oró, N. Mestres, C. Garc\'\ia, A. Pomar, B. Mart\'\inez, Spontaneous in-flight assembly of

magnetic nanoparticles into macroscopic chains. *Nanoscale*. **11**, 14194–14202 (2019).

31. S. Miyashita, Z. Nagy, B. J. Nelson, R. Pfeifer, The influence of shape on parallel self-assembly. *Entropy*. **11**, 643–666 (2009).

32. E. S. Pyanzina, A. V Gudkova, J. G. Donaldson, S. S. Kantorovich, Cluster analysis in systems of magnetic spheres and cubes. *J. Magn. Magn. Mater.* **431**, 201–204 (2017).

33. D. Zablotsky, L. L. Rusevich, G. Zvejnieks, V. Kuzovkov, E. Kotomin, Manifestation of dipole-induced disorder in self-assembly of ferroelectric and ferromagnetic nanocubes. *Nanoscale*. **11**, 7293–7303 (2019).

34. M. Cubukcu, O. Boulle, N. Mikuszeit, C. Hamelin, T. Bracher, N. Lamard, M.-C. Cyrille, L. Buda-Prejbeanu, K. Garello, I. M. Miron, O. Klein, G. de Loubens, V. V Naletov, J. Langer, B. Ocker, P. Gambardella, G. Gaudin, Ultra-Fast Perpendicular Spin-Orbit Torque MRAM. *IEEE Trans. Magn.* **54**, 1–4 (2018).

35. L. Abelmann, N. Tas, E. Berenschot, M. Elwenspoek, Self-Assembled Three-Dimensional Non-Volatile Memories. *Micromachines*. **1**, 1–18 (2010).

36. D. H. Gracias, J. Tien, T. L. Breen, C. Hsu, G. M. Whitesides, Forming electrical networks in three dimensions by self-assembly. *Science (80-. ).* **289**, 1170–1172 (2000).

**Acknowledgments:**

The authors would like to acknowledge Ir. M. Marsman, Dr. Leon Woldering and ing. Remco Sanders for conception and realisation of the setup, Prof. Andreas Manz and Prof. Gijs Krijnen for valuable advice and discussions, Proof-Reading-Service.com for carefully correcting the manuscript and the anonymous reviewers for improving the manuscript and suggesting a more elegant summation for the first equation. This work was funded by KIST Europe, under basic grant 11908. L.A., T.A.H and M.C.E generated the concept to use shape to tailor the dipolar interaction, T.A.H and P.A.L performed the experiments, all contributed substantially to the manuscript. Authors declare no competing interests. All data is available in the main text or the supplementary materials.

**Supplementary Materials:**

Videos:

<Cluster_growth_shape.mp4>
https://www.youtube.com/watch?v=8gkZvwunz04&feature=youtu.be

**Video S1:** Video recording of eight spheroids, cylinders, and spheroids with three different aspect ratios.

<Cluster_growth_number_particles.mp4>
https://www.youtube.com/watch?v=O_u7Poe2k3k&feature=youtu.be

**Video S2:** Video recording of spheroids, cylinders, and spheroids with balanced energy for the parallel and anti-parallel alignment, with 8, 12, and 16 objects.

Data:

Objects.zip: File with 3D print designs (*.STL files)

# Supplementary Material
# Three-dimensional self-assembly using dipolar interaction

L. Abelmann, T.A.G. Hageman, P.A. Löthman, Massimo Mastrangeli, and Miko C. Elwenspoek
(Dated: January 27, 2020)

## I. MATERIALS AND METHODS

Table S1 lists the dimensions of the objects used in this experiment. The STL files used for 3D printing are attached in the file `Designs.zip`.

TABLE S1: *Outer dimensions of the objects investigated, the value between brackets is the standard deviation in units of the last digit, estimated from four measurements.*

| | $\Delta E$ (μJ) | Aspect Ratio | Diameter (mm) | Height (mm) |
|---|---|---|---|---|
| Spheroid | -40 | 1.0 | 18.3(1) | 19.1(1) |
| | 0 | 1.3 | 14.6(1) | 19.1(1) |
| | +40 | 1.6 | 14.6(1) | 23.6(2) |
| Cylinder | -40 | 1.0 | 18.7(1) | 19.2(1) |
| | 0 | 1.3 | 14.8(1) | 19.2(1) |
| | +40 | 1.6 | 14.8(1) | 23.8(1) |
| Cube | -40 | 1.0 | 18.5(1) | 19.2(1) |
| | 0 | 1.3 | 14.6(1) | 19.2(1) |
| | +40 | 1.6 | 14.6(1) | 23.7(1) |

## II. FIGURES AND MOVIES

Figure S3 shows the effect of increasing amount of objects. Videos of the effect of shape (Figure S1) and the effect of the number of objects (Figure S2) are available as additional material and online (underlined links).

FIG. S1: `ClusterGrowthShape.mp4`*: Video recording of eight spheroids, cylinders, and spheroids with three different aspect ratios*

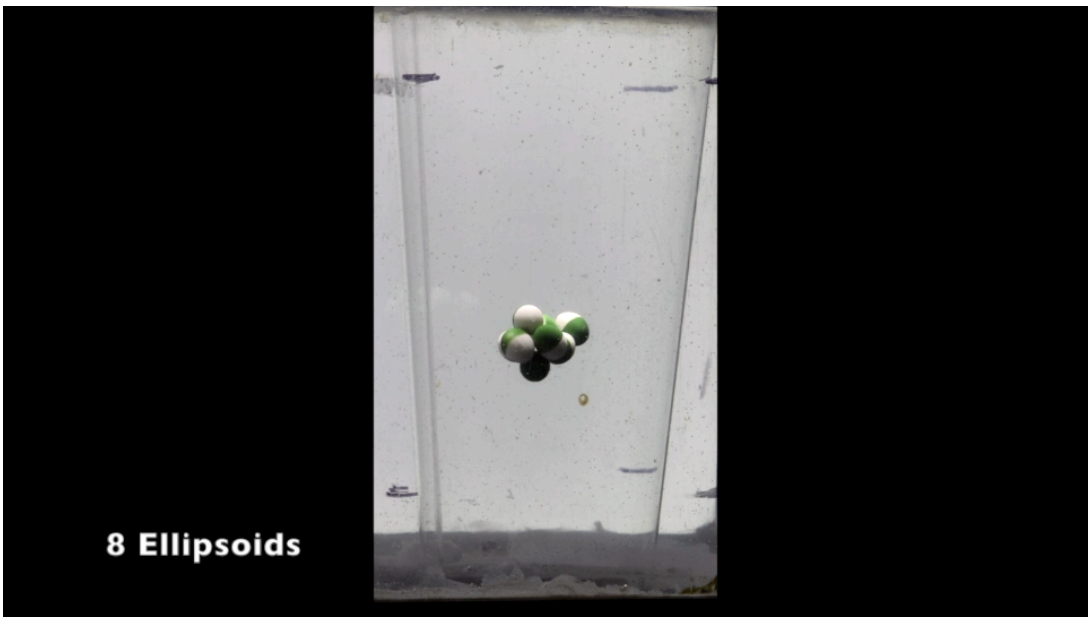


FIG. S2: `ClusterGrowthNumberParticles.mp4`*: Video recording Video recording of spheroids, cylinders, and spheroids with balanced energy for the parallel and anti-parallel alignment, with 8, 12, and 16 objects.*

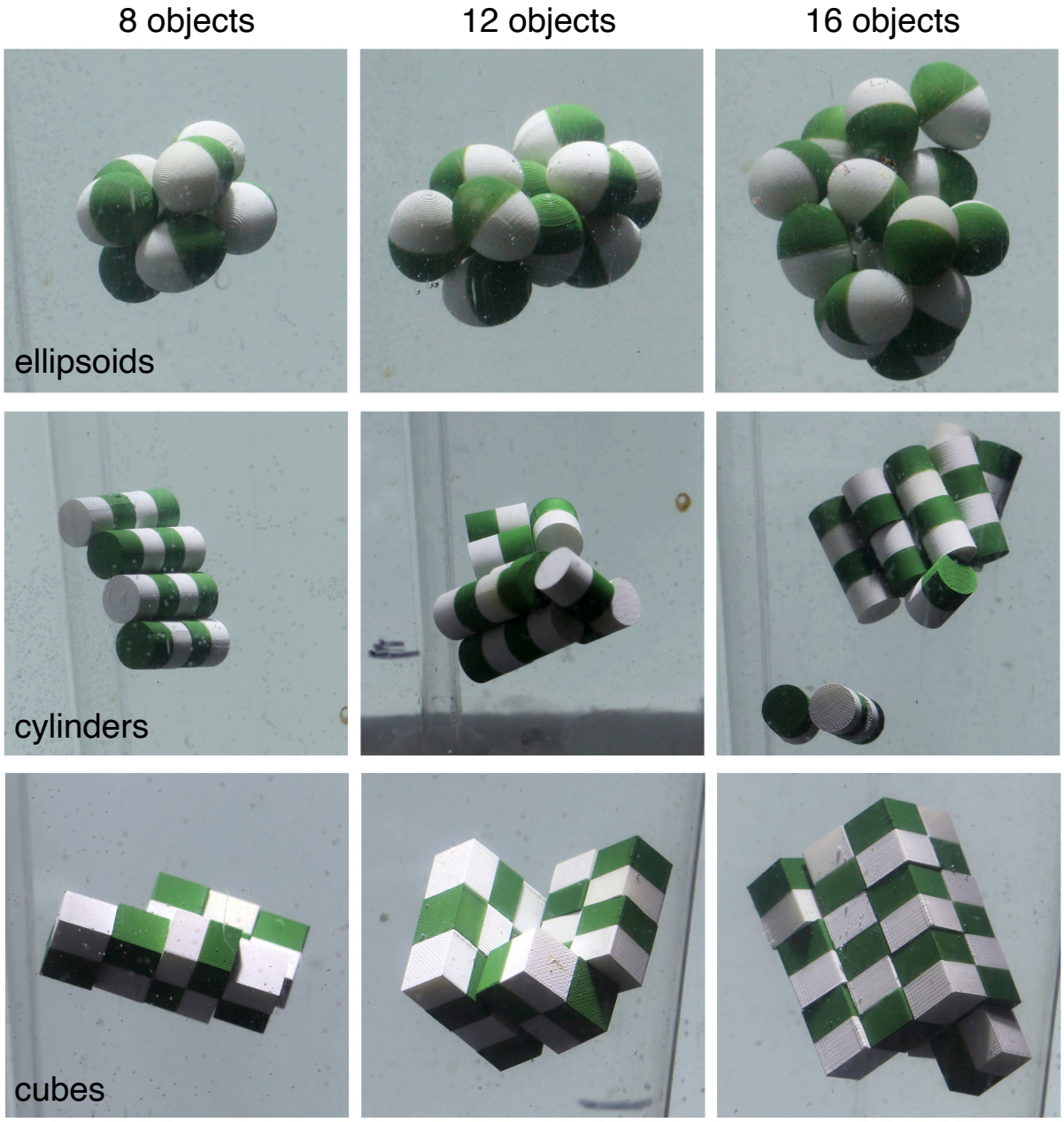


FIG. S3: . *Increasing the number of objects. Using an object shape for which the parallel and anti-parallel configuration are identical, the number of objects in the cylinder is increased from 8 to 16 (left to right). The spheroids in the top row do not form regular structure. The cylinders and cubes tend to form crystals, with an occasional "adatom" on the outside that follows a flux-closure structure.*